Delineation of freshwater zones in the shallow coastal aquifers of Ernakulam-Chettuva region, Central Kerala, India using electrical resistivity methods

PRIJU C P (cppriju@gmail.com)
Centre for Water Resources Development and Management https://orcid.org/0000-0001-5427-9359
C M Sushanth
Centre for Water Resources Development and Management
Vipin Balan P
Centre for Water Resources Development and Management

Research Article

Keywords: Saline intrusion, Coastal aquifers, Electrical resistivity methods, Ernakulam-Chettuva coast, Central Kerala, India

Posted Date: April 21st, 2021

DOI: https://doi.org/10.21203/rs.3.rs-369371/v1

Abstract

Freshwater zones in the shallow aquifers extending from Ernakulam to Chettuva region, central Kerala coast has been studied using electrical resistivity methods. Seasonal salinity patterns and hydrochemistry in the shallow aquifers in the region also has also been studied. The coastal zone is made up of shore parallel ridges and runnels formed by alternate marine trangressive and regressive events. Vertical Electrical Sounding (VES) was carried out at 33 locations in the area extending from the beach to approximately up to 10 km from the shoreline. The subsurface lithology and freshwater layers in the aquifer system was delineated from the resistivity model. The saline zones are intervening with fresh water zones at different depths along the coast. The salinity in the aquifer system seems to be either due to brackish water ingress or paleo-salinity. 107 dug wells from the study area were also monitored during 2008–2010 period in pre-monsoon, monsoon and post-monsoon seasons. The water samples collected in the post-monsoon 2008 was analysed for the physico-chemical parameters viz., pH, temperature, EC, total alkalinity, salinity, turbidity, TDS, chloride (Cl^-), total hardness, Ca^{2+}, Mg^{2+}, Na^+, K^+, CO_3^{2-}, HCO_3^-, Cl^-, SO_4^{2-}, NO_3^-N and Fe^{2+}. The pH of the water samples varied from 4.47–8.32 in the post-monsoon season and 3.5–9.21 in the pre-monsoon and 5.55–9.05 in the monsoon season. The EC values ranges from 58-4500 μ mhos/cm in the post-monsoon, 59-3753 μ mhos/cm in the pre-monsoon and 51-2637 μ mhos/cm in the monsoon season. TDS values ranges from 35-2700 mg/L in the post-monsoon, 38-21190 mg/L in the pre-monsoon and 32-1668 mg/L in the monsoon season. Hill-Piper diagram indicated Ca-HCO_3 is the dominant water type followed by Na-Cl type and Na-HCO_3 type. Other water types are Ca-Cl, Mg-HCO_3, Mg-Cl, Ca-SO_4 and $MgSO_4$.

1. Introduction

Groundwater salinization is extensive and represents a special category of groundwater pollution especially in the coastal regions. Most of the freshwater salinization along the coastal areas and oceanic islands are due to the encroachment of seawater through surface and subsurface pathways (Gingerich and Voss 2005; Post 2005; Trabelsi et al. 2007). Seawater intrusion has received wide attention in the most populated coastal areas since almost 50% of the world's total population lives within 60 km of the shoreline (Chen et al. 1997; Steinich et al. 1998; Izuka and Gingerich 1998; Salama et al. 1999; Radhakrishna, 2001; Edet and Okereke 2001; Lee et al. 2002; Cardona et al. 2004; Post 2005; Kallioras et al. 2006; Sherif et al. 2006; Bridge and Allen 2006; Feseker 2007; Tweed et al. 2007). Even though saline intrusion is a natural process, it becomes an environmental problem due to excessive pumping of fresh water from an aquifer reduces the water pressure and intensifies the effect, drawing salt water into new areas. When freshwater levels drop, the intrusion can proceed further inland until reaching the pumped well (Chandler and McWhorter 1975; Reilly and Goodman 1987; Kukillaya et al. 2004; Khan and Sapna, 2004; Pareek et al. 2006). There are different causes for the salinization of fresh water zones of aquifers; which mainly depends on local hydrogeological and geomorphic characteristics. Presence of salinity in coastal aquifers can be detected by geophysical and geochemical methods. Electrical resistivity of water bearing rocks largely depends on the amount of water saturation, the chemical composition and

temperature, and the distribution of water. Groundwater columns in the shallow coastal aquifers can be characterized into fresh water, brackish water and saline water using electrical resistivity methods, employing appropriate electrode configuration. Electrical resistivity techniques were used by many researchers for the delineation of fresh-saline water interface (Ebraheem et al. 1997; Hopkins and Richardson 1999; Tronicke et al. 1999; Edet and Okereke 2001; Lee et al. 2002; Wilson et al. 2006; Bataynch 2006; Sherif et al. 2006; Morrow et al. 2010; Mario et al. 2011; McInnis et al. 2013; Befus et al. 2014; Whitman and Yeboah-Forson 2015; Bahija et.al. 2018).

The problem of salinization of coastal aquifers in Kerala has been mainly reported from Ernakulam, Thrissur and Alleppey districts (CGWBKR 2007). In Ernakulam, seawater incursion is severe around at Chellanum and Vypin coasts. It is also found along Azhikode-Kodungallur and Vatanapally-Chavakkad-Punnayurkulam area of the coast in Thrissur district. The problem has become severe by excessive groundwater draft – Kodungallur in Thrissur district and Paraur of Ernakulam district are over-exploited and semi-critical blocks respectively (CGWBKR 2007). Brackish water intrusion through surface water bodies and tidal inlets is a major cause of increasing salinity in the lowland areas viz., Thannermukkam bund and Cherthala-Alleppey coast in Alleppey district, at Enamakkal saltwater regulator and Kole land basin in Thrissur district (Lakshminarayanan and Siva Prasad Rao 1988; Vatakkepat and Narasimha Prasad 1991; Priju et al. 2018).

The study area is part of central Kerala coast from Ernakulam (Vypin) in the south to extending upto Chettuva in the north. Geomorphologically the area is part of the back barrier-lagoon complex system flanked by Lakshadweep Sea in the western side and Vembanad lagoon and Canolly canal in the eastern side. The Vembanad backwaters and Thrissur Kol wetlands lies in the eastern side of the area drained by four rivers viz., Periyar, Chalakudy, Karuvannur and Keecheri-Puzhakkal carrying large volume of sediment load in this region. The coastal barrier land is mainly made up of sand to clayey-silty sand deposits (strandplain) with alternate ridge-runnel topography (Narayana and Priju 2006). Geologically the Warkalli and Vaikom beds (Tertiary age) underlie the strandplain deposits followed by the crystalline basement (Charnockites and hornblende biotitie-gneiss). Quilon series, a layer of lime shell bearing marine clay deposit is found pinching out within the Warkalli beds. Both Warakalli and Vaikom beds are fresh water bearing formations and consist of sandstone and conglomerate respectively.

Periyar River is the major river with a length of 244 km and basin area of 5398 km^2. Chalakudy River has a length of 130 km with a basin area of 1704 km^2. Karuvannur river has a length of 48 km with a basin area of 1054 km^2. Keecheri-Puzhakkal river has a length of 80 km with a total basin area of 635 km^2. Geologically the study area is mainly covered with paleobeach deposits (Guruvayur formation) and younger beach deposits (Kadappuram formation). It is intervened by fluvial (Periyar formation) to fluvio-marine deposits (Viyyam formation) in the northern parts of the study area. The eastern parts are covered by Charnockites and biotite gneiss with alterites (laterites).

2. Materials And Methods

Geo-electrical sounding (vertical electrical sounding) was carried out along eight east-west cross-shore traverses (A-A¢, B-B¢, C-C¢, D-D¢, E-E¢, F-F', G-G' and H-H') perpendicular to the coast line during pre-monsoon season (Figure 3). The survey was conducted applying Schlumberger electrode configuration using CRM 500 Aquameter with a maximum electrode separation (AB/2) of 100 m. VES survey was carried out at 33 stations and the apparent resistivity data was interpreted using *ZondIP* software. The seasonal water quality parameters (pH, EC, TDS, salinity and alkalinity) measured from the shallow dug wells during post-monsoon 2008, pre-monsoon 2010 and monsoon 2010 season. Laboratory analysis of the post-monsoon 2008 water samples were carried out (cations, anions, total hardness, carbonate, bicarbonate, iron, nitrate and turbidity). Water type of the post-monsoon 2008 samples were found out employing Hill-Piper diagram.

3. Results And Discussion

3.2 Water quality variations

3.2.1 pH

pH shows alkaline nature in the coastal side of the post-monsoon 2008 well water samples. It is becoming acidic towards eastern side of the study area. Acidic to neutral nature is increasing in the monsoon and pre-monsoon water samples (Figure 4). In the post-monsoon season (2008), the pH of the water samples varies from 4.47 to 8.32. pH varies from 5.55 to 9.05 in the monsoon season (2010) and varies from 3.5 to 9.21 in the pre-monsoon season (2010).

3.2.2 Temperature

In-situ measurements shows the temperature of the pre-monsoon well water samples is higher compared to monsoon (Figure 5). In the pre-monsoon 2010 season, the temperature of water samples varied from 25.33ºC to 33.71ºC. In the monsoon season the temperature of the water samples varied from 24.88ºC to 29.51ºC.

3.2.3 Total Dissolved Solids (TDS)

The TDS values are higher in the post-monsoon 2008 well water samples towards the southern part of the study area. Generally the TDS values are higher in the monsoon water samples compared with post-monsoon (Figure 6). The TDS of the water samples varied from 34.8 mg/L to 2700 mg/L in the post-monsoon 2008 season. It varies from 38 mg/L to 21190 mg/L in the pre-monsoon 2010. TDS values ranges from 32 mg/L to 1668 mg/L in the monsoon 2010 season.

3.2.4 Electrical Conductivity

The EC values are comparatively higher in the southern part of the study area compared to north in the post-monsoon 2008 (Figure 7). The EC values of the well water samples ranges from 58µS/cm to 4500µS/cm in the post-monsoon 2008 season. It varies from 51 µS/cm to 2637 µS/cm in the monsoon

season. EC values ranges from 59µcm to 3753 µS/cm in the pre-monsoon 2010 season. Higher EC values are seen in the shoreward water samples in the monsoon season.

3.2.5 Salinity

Salinity values of the well water samples are generally higher in the pre-monsoon. The salinity values of the water samples ranges from 0.03 ppt to 20.17 ppt in the pre-monsoon 2010 season. It varies from 0.02 ppt to 1.32 ppt in the monsoon 2010 season.

3.2.6 Dissolved Oxygen

During monsoon season, the DO content of the well water samples varied from 0 to 284 mg/L. In the pre-monsoon 2010 season, the DO content varied from 0.07 mg/L to 13.21 mg/L. The DO content is higher in the middle portions of the study area in the pre-monsoon season compared to monsoon season in which higher in the southern parts (Figure 9).

Fig.9 DO content of the water samples in the pre-monsoon and monsoon season

3.2.7 Total Hardness

The total hardness values of the well water samples varied from 15 mg $CaCO_3$/L to 475 mg $CaCO_3$/L in the post-monsoon season. TH is higher towards the southern and western part of the study area compared to northern and eastern part (Figure 10).

3.2.8 Calcium (Ca^{2+})

The calcium content of the well water samples in post-monsoon 2008 varied from 2 to 90 mg/L. Calcium content is higher shoreward and towards southern part of the study area (Figure 11).

3.2.9 Magnesium (Mg^{2+})

The magnesium content of the well water samples varies from 1.1 mg/L to 92.7 mg/L in the post-monsoon 2008. Magnesium content is higher towards the southern and northern part of the study area (Figure 12).

3.2.10 Sodium (Na^{+})

The sodium content of the well water samples varied from 3.1 mg/L to 710 mg/L in the post-monsoon 2008. Sodium content is found higher in the southern part of the study area (Figure 12).

3.2.11 Potassium (K^{+})

The potassium content of the well water samples varied from 0.65 mg/L to 43 mg/L in the post-monsoon 2008 season. Potassium content is higher in the southern part of the study area compared to northern

part (Figure 13).

3.2.12 Carbonate (CO_3^{2-})

The carbonate content of the well water samples varied from 0 to 24 mg/L in the post-monsoon 2008 season. Carbonate content is higher in the middle part of the study area compared to the northern and southern parts (Figure 14).

3.2.13 Bicarbonate (HCO_3^-)

The bicarbonate content of the well water samples varied from 7 mg/L to 734 mg/L in the post-monsoon 2008 season. Bicarbonate content is higher in the southern part of the study area compared to the northern part (Figure 15).

3.2.14 Total Alkalinity (TA)

The total alkalinity in the well water samples varied from 6 to 602 mg CO_3/L in the post-monsoon 2008 season. Total alkalinity is higher in the southern part of the study area compared to the northern part (Figure 16).

3.2.15 Iron (Fe)

The Fe content in the well water samples varies from 0 to 9.22 mg/L in the post-monsoon 2008 season. Fe content is higher in the middle and southern part of the study area compared to the northern part (Figure 17).

3.2.16 Chloride (Cl^-)

The chloride content in the well water samples varied from 1.27 mg/L to 186 mg/L in the post-monsoon 2008 season. Chloride content is more or less uniform, but slight increase is noted in the northern and middle part of the study area (Figure 18).

3.2.17 Sulfate (SO_4^{2-})

The sulfate content in the well water samples varies from 0 to 161 mg/L in the post-monsoon 2008 season. Sulfate content is generally higher in the eastern part of the study area compared to the western part (Figure 19).

3.2.18 Nitrate (NO_3^-N)

The nitrate content in the well water samples varied from 0.01 mg/L to 6.05 mg/L in the post-monsoon 2008 season. The nitrate content shows higher values in the northern and southern part of the study area as well as eastern part in the middle portion (Figure 20).

3.2.19 Turbidity

The turbidity of the well water samples varied from 0 to 11 mg/L in the post-monsoon 2008 season (Figure 21).

3.3 Hill-Piper Diagram

Hill-piper diagram of the post-monsoon 2008 water samples was plotted and 8 water types were found. Majority of the water samples are Ca-HCO_3 type (55 Nos) followed by Na-Cl type (19 Nos). It is followed with Na-HCO_3 type (13 Nos.). 6 samples show CaCl type and 5 samples show Mg-HCO_3 type. Two samples each are $CaSO_4$ type and MgCl water type. One sample belongs to $MgSO_4$ type.

3.4 Geophysical Investigation

Geophysical investigation (VES) was carried out in eight cross-shore traverses in the study area with schlumberger configuration. Eight cross-shore profiles were constructed. Maximum current electrode separation is 100 m.

3.4.1 Vertical Electrical Sounding

Vertical Electrical Soundings were carried out at 43 locations. It is found that majority of the curves are Q-type (16 nos) followed by H-type curves (13 nos). K-type curves are obtained from 3 locations. KA-type and QA-type curves are seen from one locations each.

3.4.2 Pseudo section

A total of 33 soundings (VES) were carried out in different stretches along the coast. Majority of the curves obtained are Q-type (VES-7, VES-8, VES-11, VES-12, VES-16, VES-17, VES-22, VES-23, VES-24, VES-26, VES-27, VES-32, VES-33, VES-46, VES-47, VES-48), followed by H-type curves (VES-1, VES-2, VES-4, VES-6, VES-9, VES-10, VES-14, VES-15, VES-18, VES-19, VES-20, VES-29, VES-34). K-type curve was obtained at three locations (VES-3, VES-13, VES-25), KA-type (VES-30) and QA type curves (VES-31) in one locations each. The selected model curves obtained and pseudo sections are shown in the figures. The resistivity parameters obtained by matching the field and master curves (*ρ, h & d)* are given in the Table 1.

Table 1: Resistivity parameters (*ρ, h & d)* interpreted from the field curves

VES No.	No. of Layers	Apparent Resistivity, ρ (Ωm)				Thickness, h (m)				Total Thickness, *d* (m)
		ρ1	*ρ2*	*ρ3*	*ρ4*	*h1*	*h2*	*h3*	*h4*	
VES-1	3	288	19	4048	-	1.18	13.28	∞	-	14.46
VES-2	3	1577	13	3077	-	0.96	16.03	∞		16.99
VES-3	3	79	1906	4	-	0.40	0.48	∞		0.88
VES-4	3	2982	25	400	-	1.82	7.29	∞		9.11
VES-6	3	389	16	234	-	1.38	0.58	∞		1.96
VES-7	3	4309	71	0	-	1.91	11.69	∞		13.6
VES-8	3	4612	718	1	-	3.59	5.37	∞		8.96
VES-9	3	639	1	2	-	0.61	0.45	∞		1.05
VES-10	3	638	2	1827	-	3.56	8.66	∞		12.22
VES-11	3	1084	23	5	-	0.68	7.04	∞		7.72
VES-12	3	263	1	0	-	1.40	15.90	∞		17.3
VES-13	3	944	4920	11	-	0.21	3.37	∞		3.79
VES-14	3	355	3	5	-	2.11	10.06	∞		12.17
VES-15	3	6518	4	265	-	6.24	3.63	∞		9.87
VES-16	3	7811	297	0	-	5.36	8	∞		13.36
VES-17	3	4445	229	7	-	5.67	60.98	∞		72.32
VES-18	3	637	75	176	-	2.57	10.88	∞		13.45
VES-19	3	477	21	2269	-	2.79	39.13	∞		41.92
VES-20	3	263	21	184	-	0.83	21.53	∞		22.36
VES-22	3	545	31	6	-	2.32	7.53	∞		9.85
VES-23	3	6	1	1	-	1.33	0.56	∞		1.89
VES-24	3	183	15	2	-	0.7	6.36	∞		7.06
VES-25	3	119	2794	68	-	0.05	5.50	∞		5.55
VES-26	3	237	32	10	-	1	5.90	∞		6.90
VES-27	4	5841	265	7	0	9.22	17.38	29	∞	55.60
VES-29	3	19	2	64	-	3.03	57.37	∞		60.4
VES-30	4	514	9832	7	202	0.11	4.83	21.60	∞	26.54
VES-31	4	598	10	1	649	1.71	5.38	11.47	∞	18.56
VES-32	3	362	112	1	-	0.89	2.09	∞		2.98
VES-33	3	924	7	1	-	1.94	8.67	∞		10.61
VES-34	3	1210	1	668	-	4.42	4.84	∞		9.26
VES-46	3	202	3	0	-	1.85	25.28	∞		27.13
VES-47	4	216	88	6	0	0.86	2.23	18.37	∞	21.46
VES-48	4	341	28	9	2	0.81	3	6.09	∞	9.9

3.4.3 Cross sectional profiles

Eight cross-sectional profiles were represented connecting the VES'es perpendicular to the coastline. The profiles are A-A', B-B', C-C', D-D', E-E', F-F', G-G' and H-H'. The profiles indicates variations in apparent resistivity across the coast from beach to landward direction. The profile A-A' indicate the presence of high resistive zone in the seaward direction. Low resistive saline zone is indicated towards east and also shows a thickening trend.

The profile B-B' shows a similar trend with high resistive zone in the shoreward direction and low resistive zone in the landward direction. The presence of freshwater lens in the shoreward region and saline wedge in the landward region is prominent.

The profile C-C' indicate the presence of high resistive freshwater zone in the western side in the shoreward zone and low resistive zone towards the landward side. Low resistive saline wedge is seen towards depth.

In the profile D-D', the high resistive zone is seen in the shoreward side with a saline wedge in the bottom extending towards landward side towards east.

The profile E-E' shows the high resistive freshwater lens in the middle of the land area and low resistive zones in the eastward and westward direction. The saline wedge is at depth in the shoreward direction.

In the profile F-F', a clear high resistive freshwater zone is found in the landward side whereas the low resistive saline zones are seen towards the shoreward direction.

In the profile G-G' high resistive zones are seen in the topmost portions and towards east. Saline zones are seen towards depth and in the shoreward direction.

In the profile H-H'. high resistive zones are seen in the western side into the middle and is thinning towards east. Saline wedge is seen in the bottom and towards the eastern parts.

4. Conclusions

Spatially, it is observed that in majority of the areas, brackish water intrusion into the freshwater aquifers is the major reason for salinity. The seasonal variation in TDS, salinity and anion content is influenced by the seasonal riverine and tidal flux. In some of the areas along the coast where sand ridges are predominant, freshwater aquifers are not affected by saline water intrusion. Hill-piper diagram of the well water samples indicates the presence of dominant bicarbonate type (Ca-HCO_3) water followed by NaCl type and Na- HCO_3 type water. The presence of Q-type curve in most of the locations of resistivity sounding indicate the presence of saline water upconing. Presence of H-type curve in rest of the locations indicate fresh water zones towards depth. Cross-sectional profiles indicates variations in apparent resistivity across the coast from beach to landward direction. The profiles indicate the presence of high resistive zone in the seaward direction at most of the places indicating the freshwater lens in the seaward zone. Low resistive saline zone is indicated towards east and also shows a thickening trend due to saline water upconing.

Declarations

Acknowledgement

CPP thank Department of Science and Technology (DST), New Delhi for research funding (Project No.SR/FTP/ES-43/2007).

Funding (information that explains whether and by whom the research was supported):

This work was financially supported by Department of Science and Technology (DST), New Delhi (Project No.SR/FTP/ES-43/2007)

Conflicts of interest/Competing interests (include appropriate disclosures):

No conflict of interest or competing interests

Availability of data and material (data transparency):

The data was collected from the field-primary data-which is available

Code availability (software application or custom code):

Not applicable

Authors' contributions (optional: please review the submission guidelines from the journal whether statements are mandatory):

Not applicable

References

Bahija A, Fouad A, Mohamed C, Mohamed S (2018) Assessment of saltwater contamination extent in the coastal aquifers of Chaouia (morocco) using the electric recognition. J of Hydrol 566: 363-376

Bataynch AT (2006) Use of electrical resistivity methods for detecting subsurface fresh and saline water and delineating their interfacial configuration: a case study of the eastern Dead sea coastal aquifers, Jordan. Hydrogeol J 14:1277-1283

Befus KM, Cardenas MB, Tait DR, Erler DV (2014) Geoelectrical signals of geologic and hydrologic processes in a fringing reef lagoon setting. J of Hydrol 517:508-520

Bridge DW, Allen DM (2006) An investigation into the effects of diffusion on salinity distribution beneath the Fraser river delta. Hydrogeol J 14: 1423-1442

Cardona A, Carrillo-Rivera JJ, Huizar-Alvarez R, Graniel-Castro E (2004) Salinization in coastal aquifers of arid zones: an example from Santo Domingo, Baja California Sur, Mexico. Environ Geol 45:350-366

CGWBKR (2007) **Hydro Geological Conditions of Kerala** http://cgwb.gov.in/KR/

Chandler RL, McWhorter DB (1975) Upconing of saltwater-freshwater interface beneath a pumping well. Groundwater 13:354-359

Chen H, Zhang Y, Wang X, Ren Z, Li L (1997) Salt-water intrusion in the lower reaches of the Weihe river, Shandong Province, China. Hydrogeol J 5(3):82-88

CWRDM (1984) Trichur coastal wells water quality. Report No.GW/BD-47/84. Centre for Water Resources Development and Management, Kozhikode, Kerala

Ebraheem A-AM, Senosy MM, Dahab KA (1997) Geoelectrical and hydrogeochemical studies for delineating groundwater contamination due to salt-water intrusion in the northern part of the Nile delta, Egypt. Ground Water 35:216-222

Edet AE, Okereke CS (2001) A regional study of saltwater intrusion in southeastern Nigeria based on the analysis of geoelectrical and hydrochemical data. Environ. Geol 40:1278-1289

Feseker T (2007) Numerical studies on saltwater intrusion in a coastal aquifer in northwestern Germany. Hydrogeol J 15: 267-279

Gingerich SB and Voss CI (2005) Three-dimensional variable-density flow simulation of a coastal aquifer in southern Oahu, Hawaii, USA. Hydrogeol J, 13: 436-450

Hopkins DG, Richardson JL (1999) Detecting a salinity plume in an unconfined sandy aquifer and assessing secondary soil salinization using electromagnetic induction techniques, North Dakota, USA. Hydrogeol J, 7:380-392

Izuka SK, Gingerich SB (1998) Estimation of the depth to the fresh-water/salt-water interface from vertical head gradients in wells in coastal and island aquifers. Hydrogeol J, 6:365-373

Joseph S, Thrivikramaji KP (2002) Kayals of Kerala coastal land and implication to Quaternary sea level changes. *In:* Narayana, A.C. Ed., Late Quaternary Geology of India and Sea level changes, Mem. Geol. Soc. India, 51-64

Kallioras A, Pliakas F, Diamantis I (2006). Conceptual model of a coastal aquifer system in northern Greece and assessment of saline vulnerability due to seawater intrusion conditions. Environ Geol., 51: 349-361

Khan AB, Sapna PV (2004) Groundwater salinization in different aquifers-A case study. Jour. Geol. Soc. India 63(2): 183-190

Kukillaya JP, Padmanabhan K, Radhakrishnan K (2004) Occurrence of Brackish groundwater in fractured hard rock aquifers of Puzhakkal-Avanur area in Thrissur, Kerala. Jour. Geol. Soc. India 64 (1):32-42

Lakshminarayanan P, Siva Prasada Rao GVVRG (1988) Coastal Kerala groundwater project – Detailed hydrogeological studies in the Kole land basin. Central Ground Water Board, Kerala region (CGWBKR), Report no.38

Lee S, Kim K, Ko I, Lee S, Hwang H (2002) Geochemical and geophysical monitoring of saline water intrusion in Korean paddy fields. Environ. Geochemistry and Health 24:277-291

Mario Z, Joan B, Rogelio L, Xavier MP (2011) Electrical methods (VES and ERT) for identifyign, mapping and monitoring different saline domains in a coastal plain region (Alt Emporda, Northern Spain). J of Hydrol 409:407-422

McInnis D, Silliman S, Boukari M, Yalo N, Orou-Pete S, Fertenbaugh C, Sarre K Fayomi, H (2013) Combined application of electrical resistivity and shallow groundwater sampling to assess salinity in a shallow coastal aquifer in Benin, West Africa. J of Hydrol 505:335-345

Morrow FJ, Ingham MR McConchie, JA (2010) Monitoring of tidal influences on the saline interface using resistivity traversing and cross-borehole resistivity tomography. J. of Hydrol 389:69-77

Narayana AC, Priju CP (2006) Landform and shoreline changes inferred from satellite images along the Central Kerala coast, India. Jour. Geol. Soc. India 68(1):35-49

Pareek N, Jat MK, Jain SK (2006). The utilization of brackish water, protecting the quality of the upper fresh water layer in coastal aquifers. Environmentalist 26:237-246

Post VEA (2005) Fresh and saline groundwater interaction in coastal aquifers: Is our technology ready for the problems ahead?. Hydrogeol J 13:120-123

Priju CP, Nebin PJ, Jiby F, Vipin BP, Subin Sankar TP, Narasimha Prasad NB (2018) Fresh-saline water interface in the shallow coastal aquifers of Cherthala-Alappuzha coast: Application of electrical resistivity techniques. Hydrol J 40 &41 (1-4):16-27

Radhakrishna I (2001) Saline fresh water interface structure in Mahanadi delta region, Orissa, India. Environ Geol 40(3): 369-380

Reilly TE, Goodman AS (1987) Analysis of saltwater upconing beneath a pumping well. J. Hydrol 89:169-204

Salama RB, Otto CJ, Fitzpatrick RW (1999) Contributions of groundwater conditions to soil and water salinization. Hydrogeol J 7:46-64

Sherif M, El Mahmoudi A, Graamoon H, Kacimov A, Akram S, Ebraheem A, Shetty, A (2006) Geoelectrical and hydrogeochemical studies for delineating seawater intrusion in the outlet of Wadi Ham, UAE. Environ Geol 49:536-551

Steinich B, Escolero O, Marin LE (1998) Salt-water intrusion and nitrate contamination in the valley of Hermosillo and El Sahuaral coastal aquifers, Sonora, Mexico. Hydrogeol J 6:518-526

Trabelsi R, Zairi M, Dhia HB (2007) Groundwater salinization of the Sfax superficial aquifer, Tunisia. Hydrogeol J (online version) DOI 10.1007/s10040-007-0182-0

Tronicke J, Blindow N, Groß R, Lange MA (1999) Joint application of electrical resistivity- and GPR-measurements for groundwater exploration on the island of Spiekeroog-northern Germany. J of Hydrol 223:44-53

Tweed SO, Leblanc M, Webb JA, Lubezynski MW (2007) Remote sensing and GIS for mapping groundwater recharge and discharge areas in salinity prone catchments, southeastern Australia. Hydrogeol J 15:75-96

Vatakkepat H, Narasimha Prasad NB (1991) Salinity of groundwater in the Kole lands of Trichur district, Kerala. Proc. Sem. Groundwater Development and Management in irrigation and other water sectors, CWRDM, Kozhikode pp 235-242

Whitman D, Yeboah-Forson A (2015) Electrical resistivity and porosity structure of the upper Biscayne Aquifer in Miami-Dade County, Florida. J of Hydrol 531:781-791

Wilson SR, Ingham M McConchie JA (2006) The applicability of earth resistivity methods for saline interface definition. J Hydrol 316 (1-4):301-312

Figures

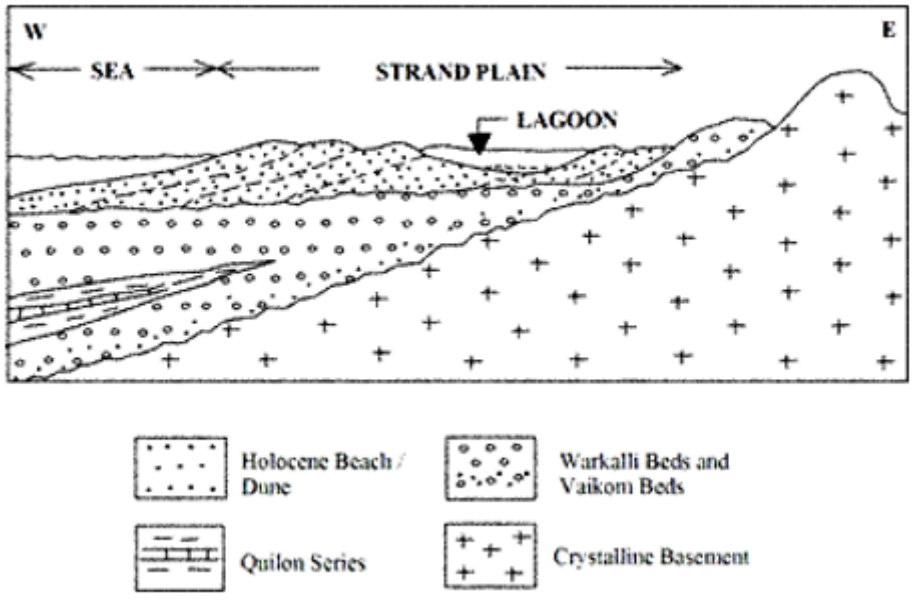

Figure 1

Simplified geologic cross-section of central Kerala coast, showing Holocene beach/dune sediments (Joseph and Thrivikramaji 2002)

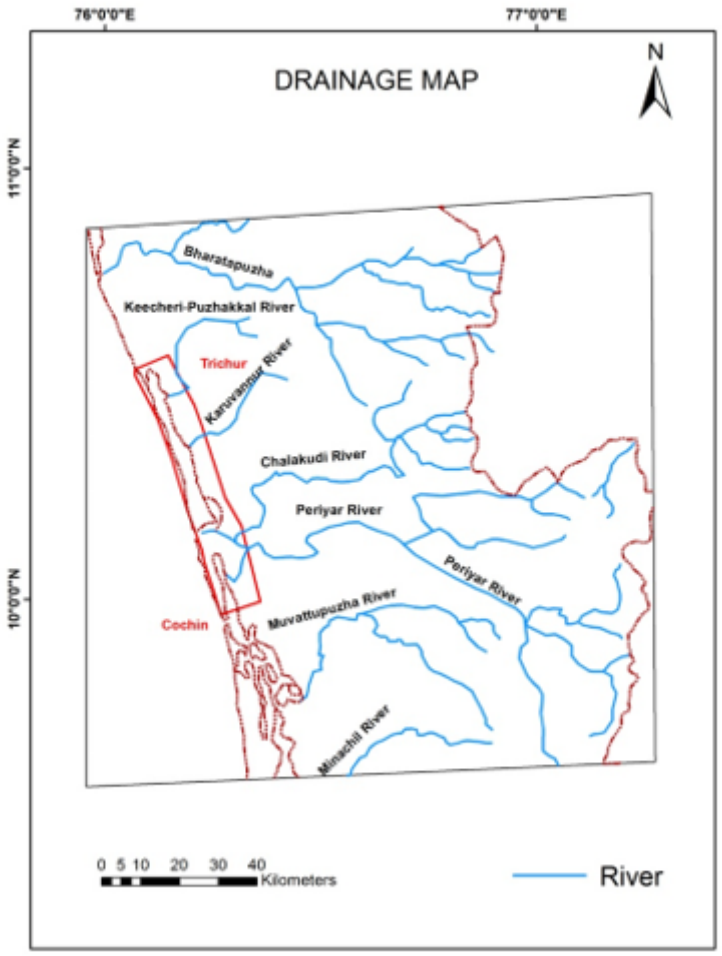

Figure 2

Drainage map of the study area

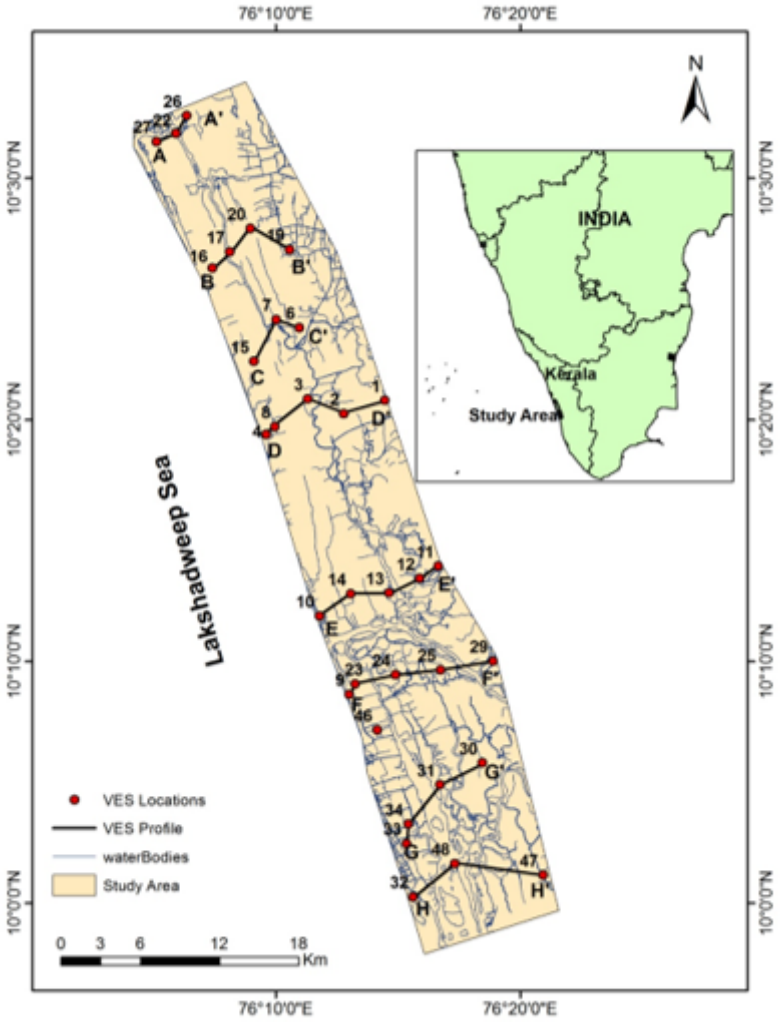

Figure 3

Study area showing VES locations and cross sectional profiles (A-A', B-B',C-C',D-D',E-E',F-F',G-G',H-H')

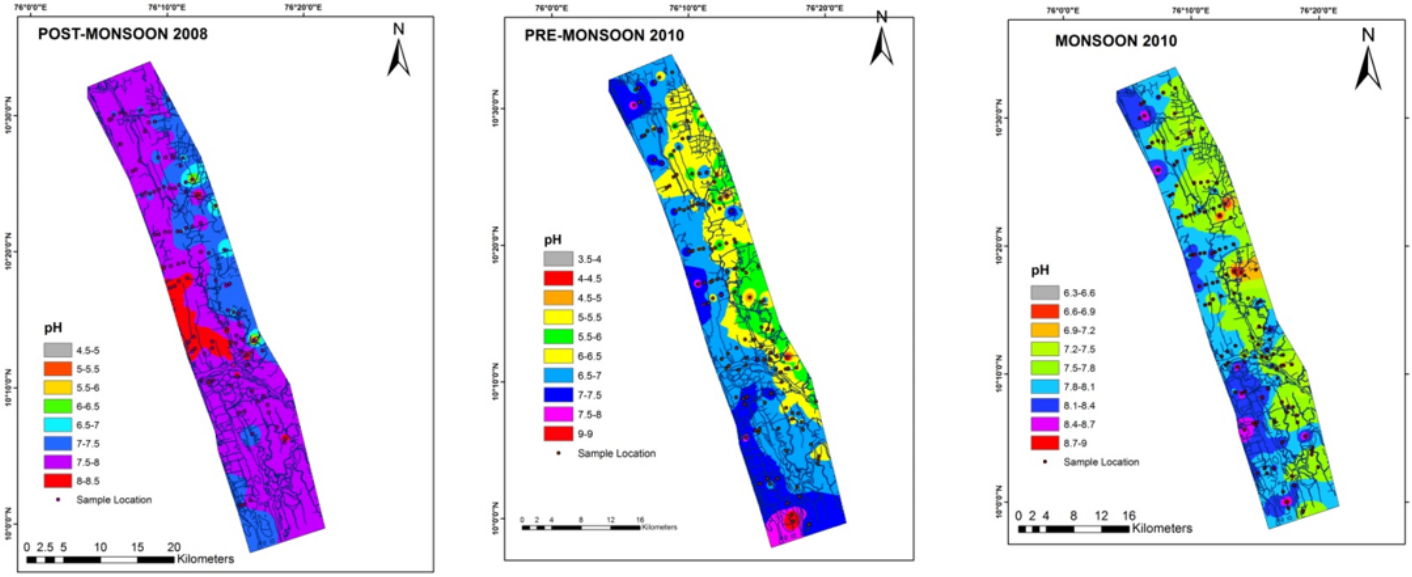

Figure 4

pH of the water samples in the pre-monsoon, monsoon and post-monsoon season

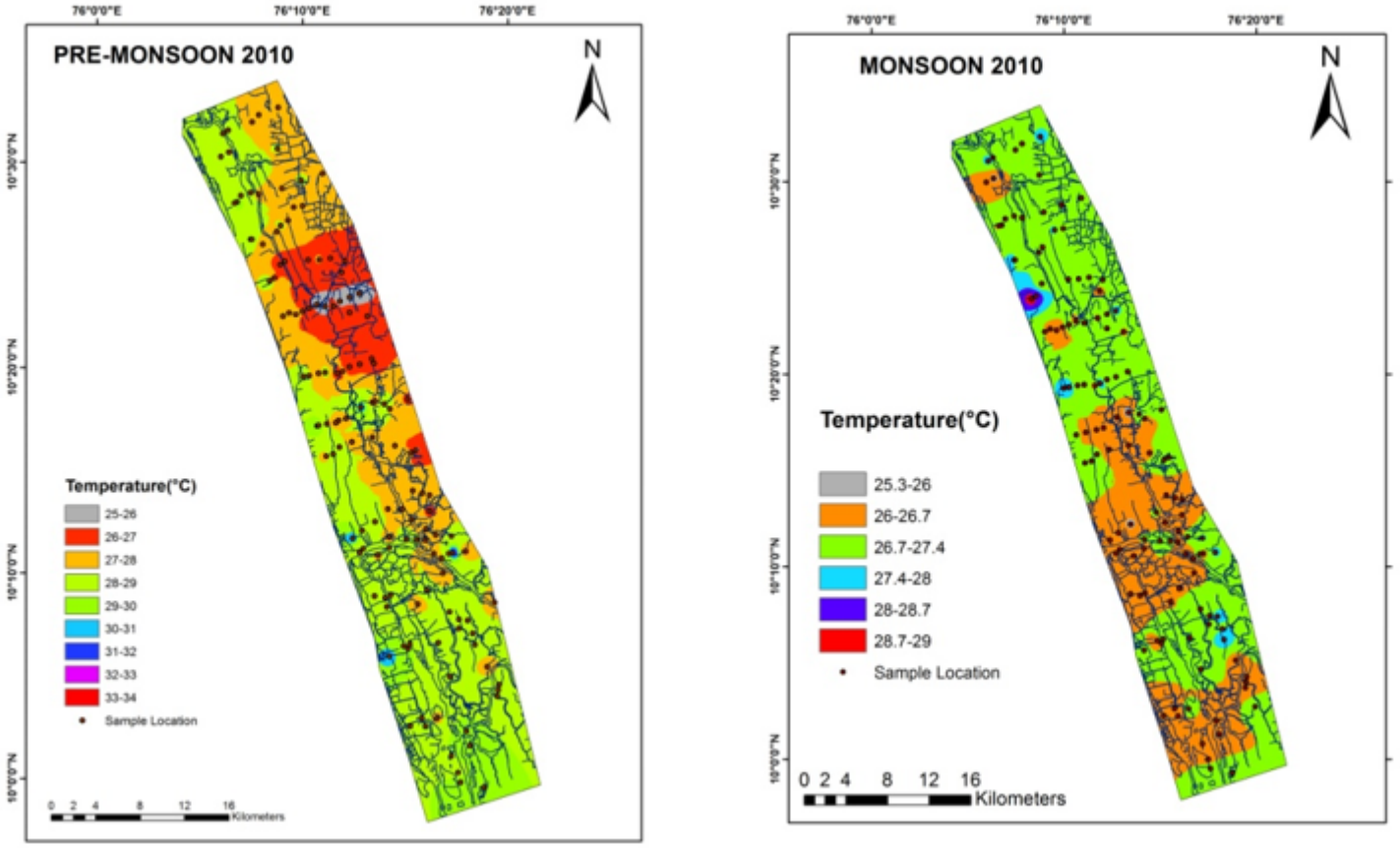

Figure 5

Temperature of the water samples in the pre-monsoon and monsoon

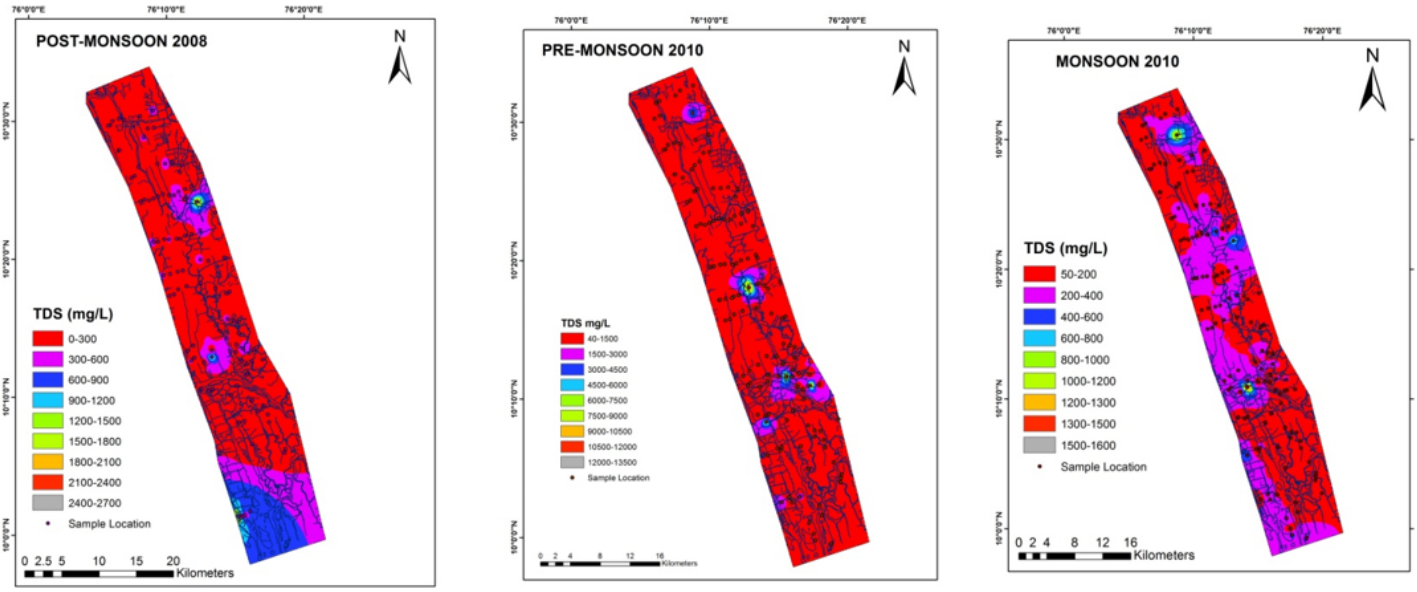

Figure 6

TDS values of the water samples in the pre-monsoon, monsoon and post-monsoon season

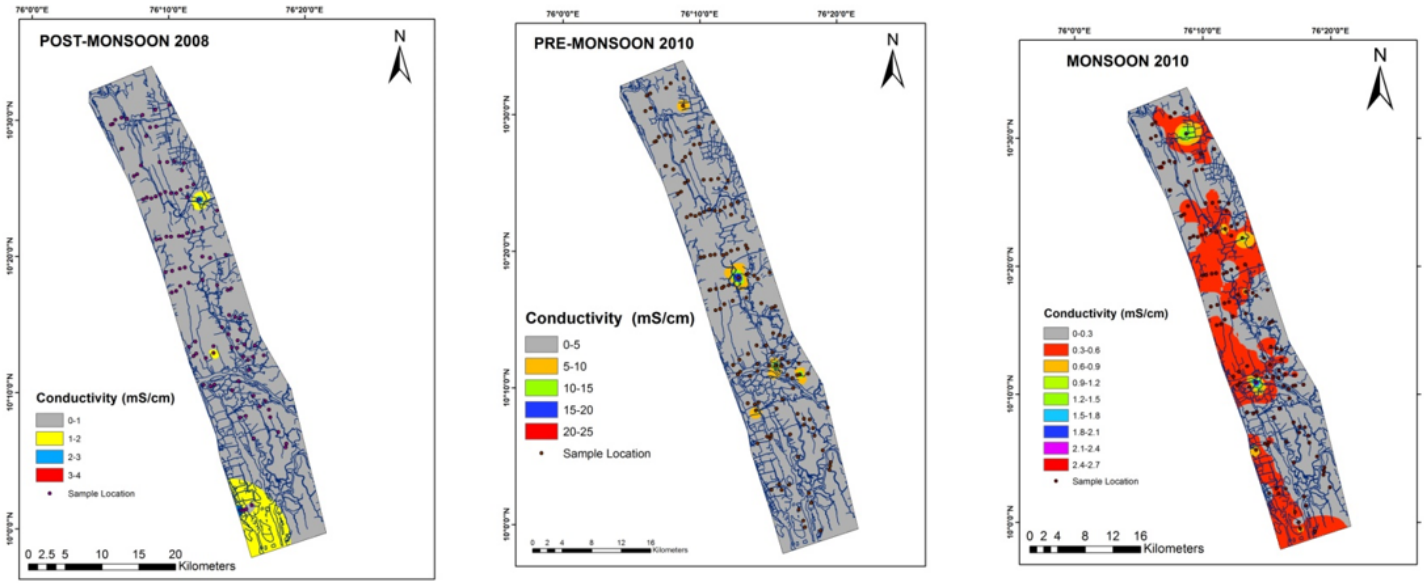

Figure 7

EC of the water samples in the pre-monsoon, monsoon and post-monsoon season

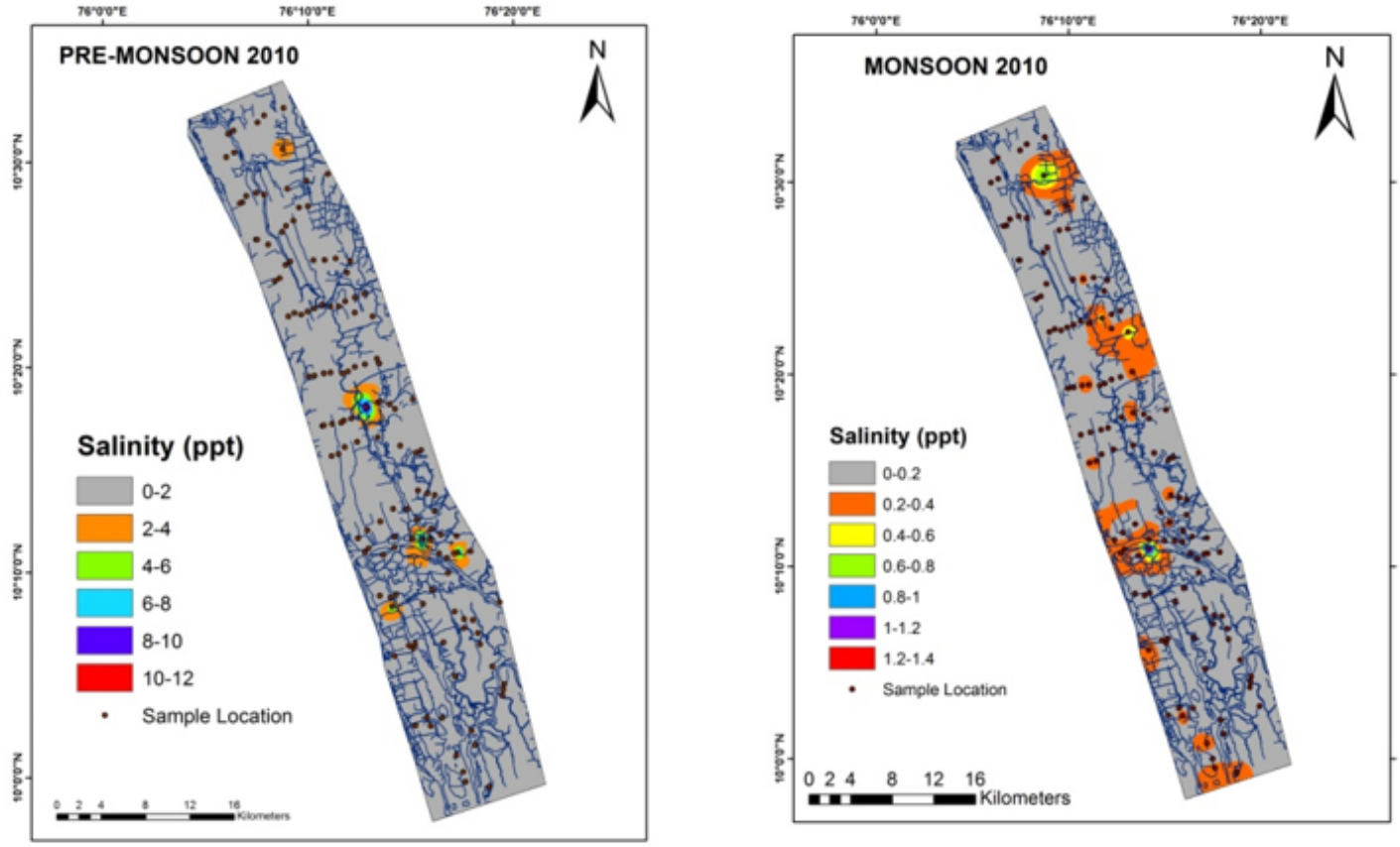

Figure 8

Salinity values of the water samples in the pre-monsoon and monsoon season

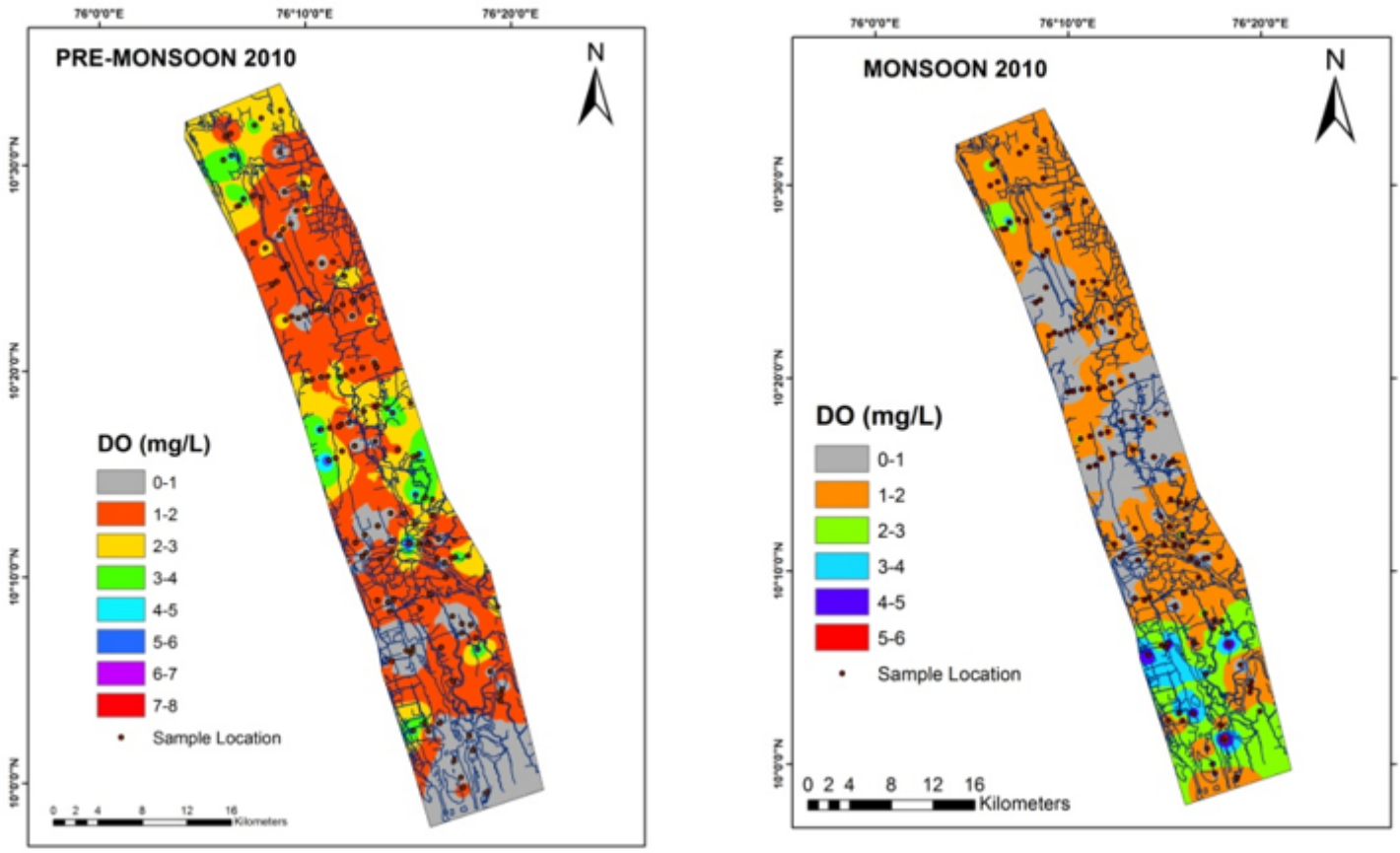

Figure 9

DO content of the water samples in the pre-monsoon and monsoon season

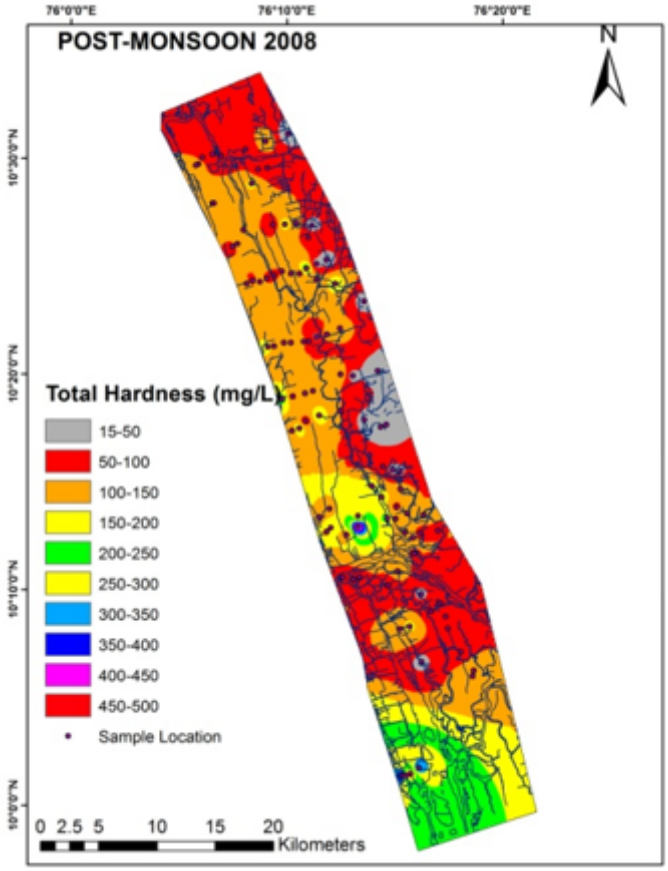

Figure 10

Total Hardness (TH) of the water samples in the post-monsoon season

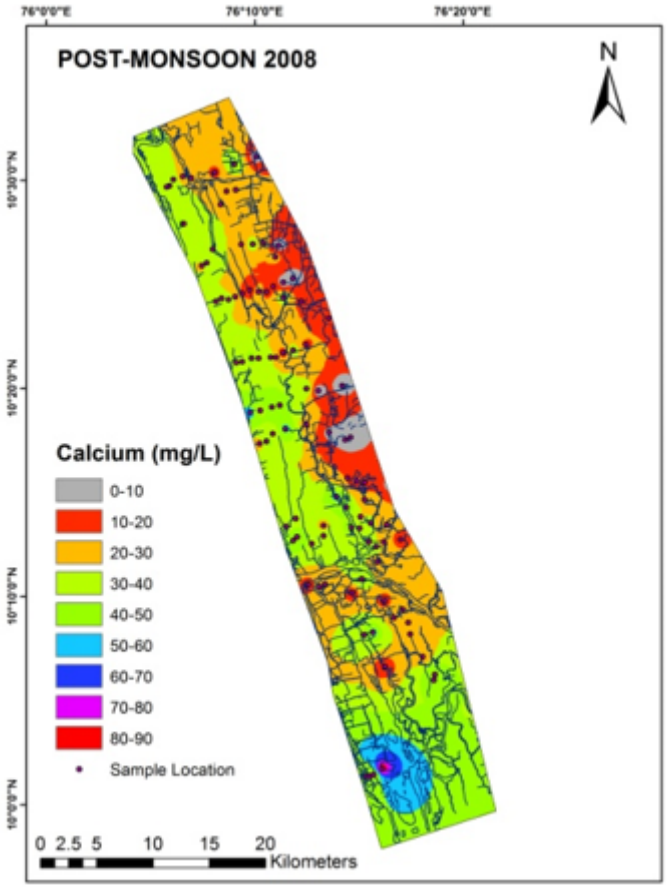

Figure 11

Ca content of the water samples in the post-monsoon season

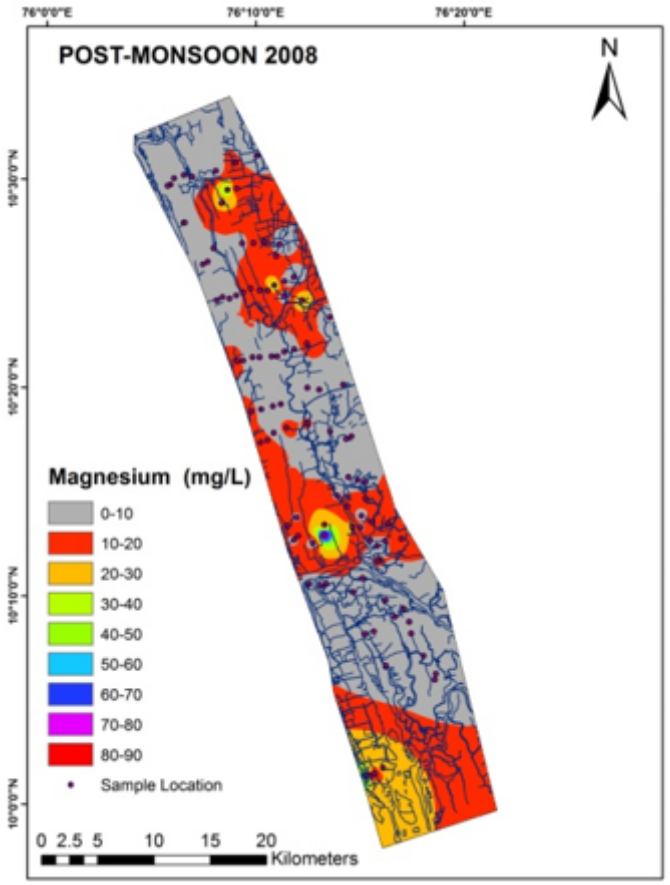

Figure 12

Mg content of the water samples in the post-monsoon season

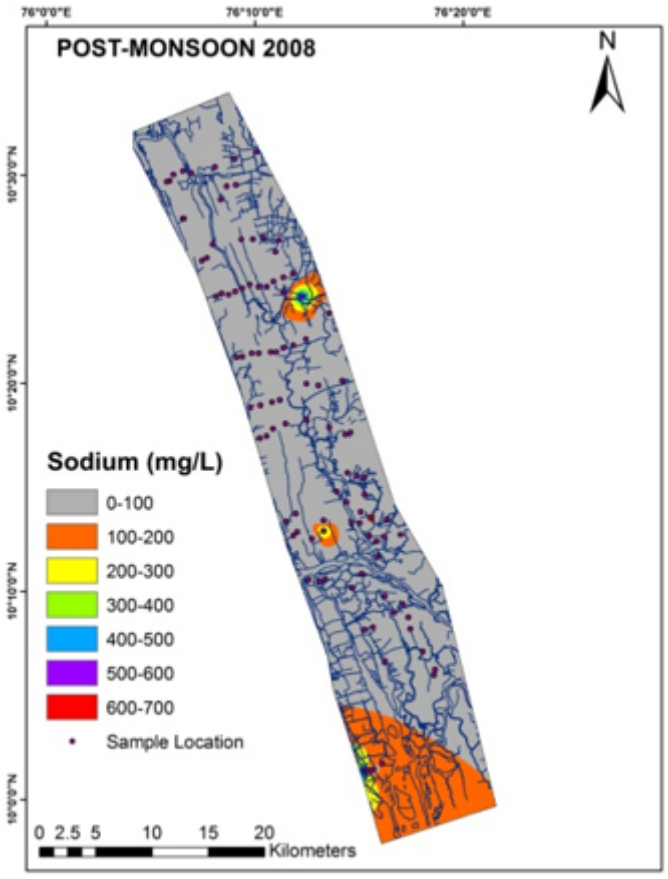

Figure 13

Mg content of the water samples in the post-monsoon season

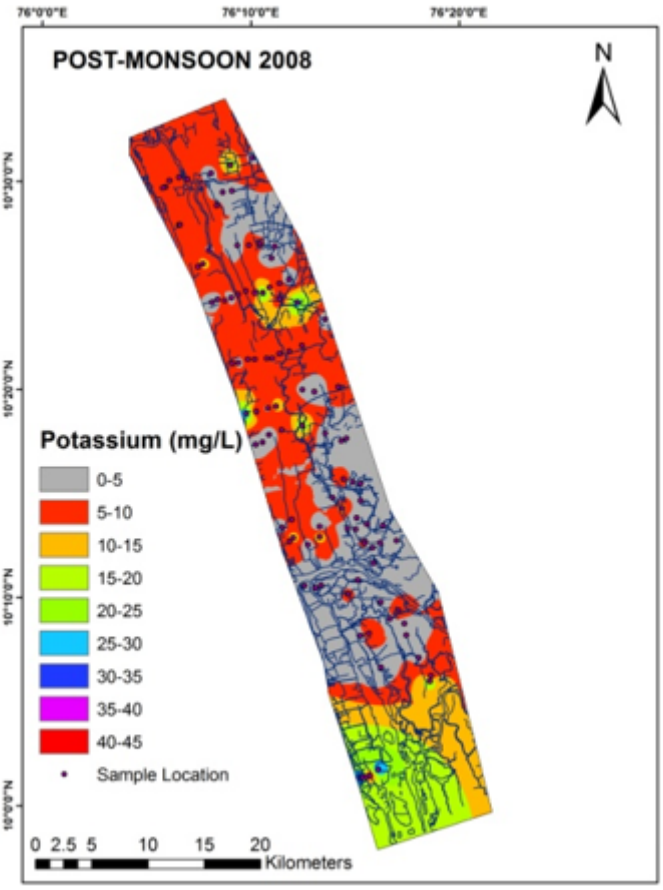

Figure 14

Potassium (K+) content of the water samples in the post-monsoon season

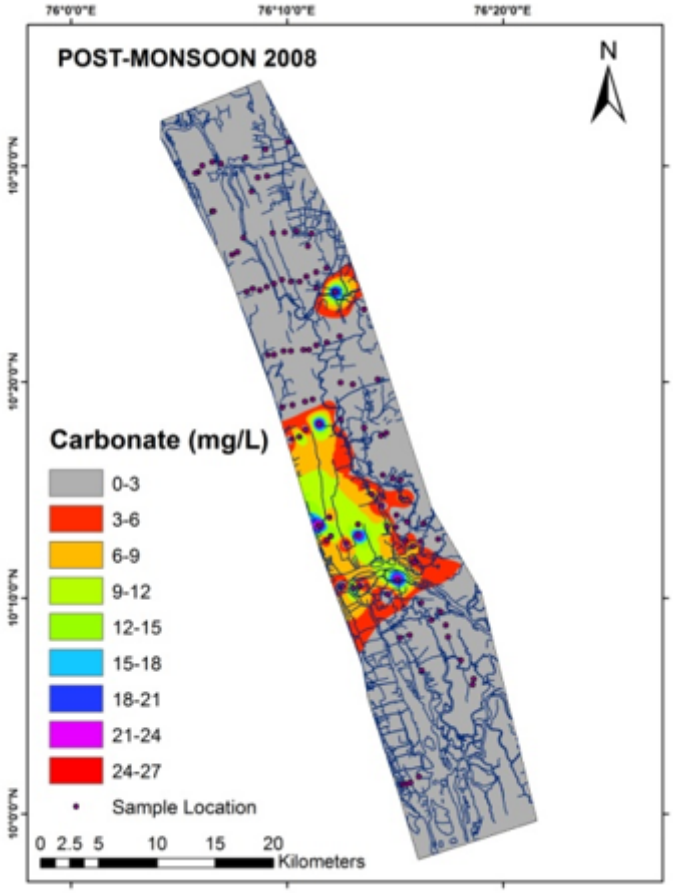

Figure 15

Carbonate (CO32-) content of the water samples in the post-monsoon season

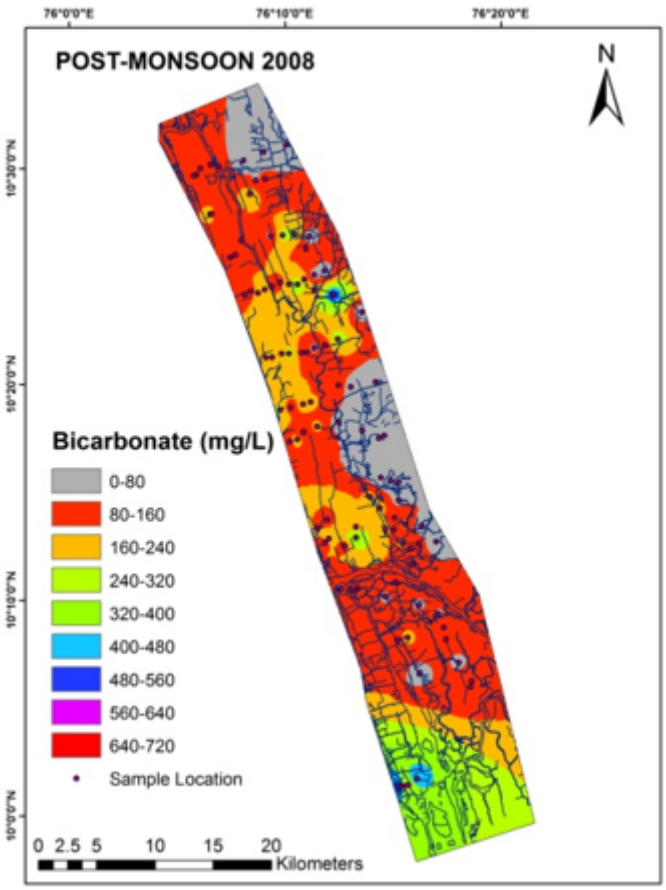

Figure 16

Bicarbonate (HCO3-) content of the water samples in the post-monsoon season

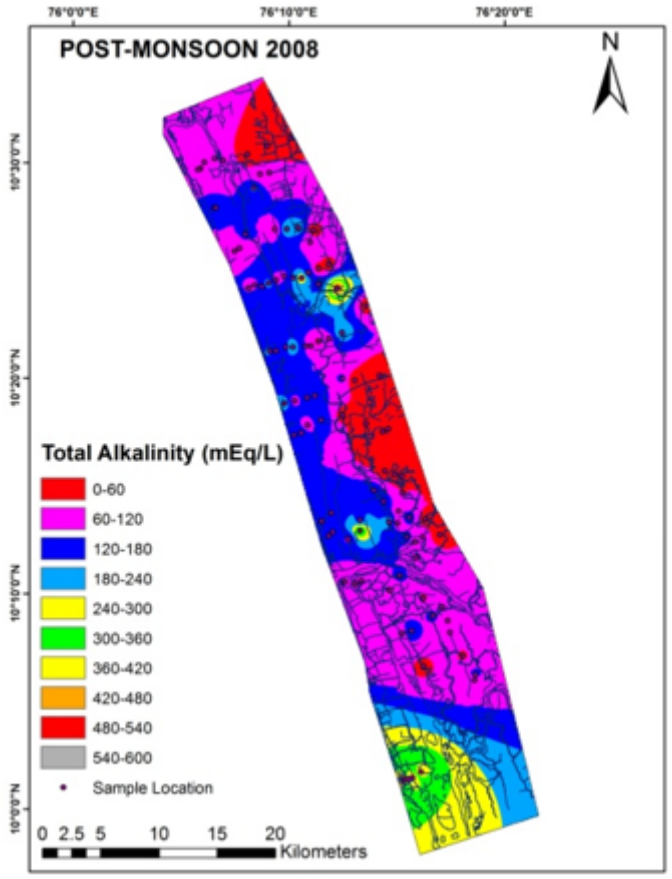

Figure 17

Total Alkalinity (TA) of the water samples in the post-monsoon season

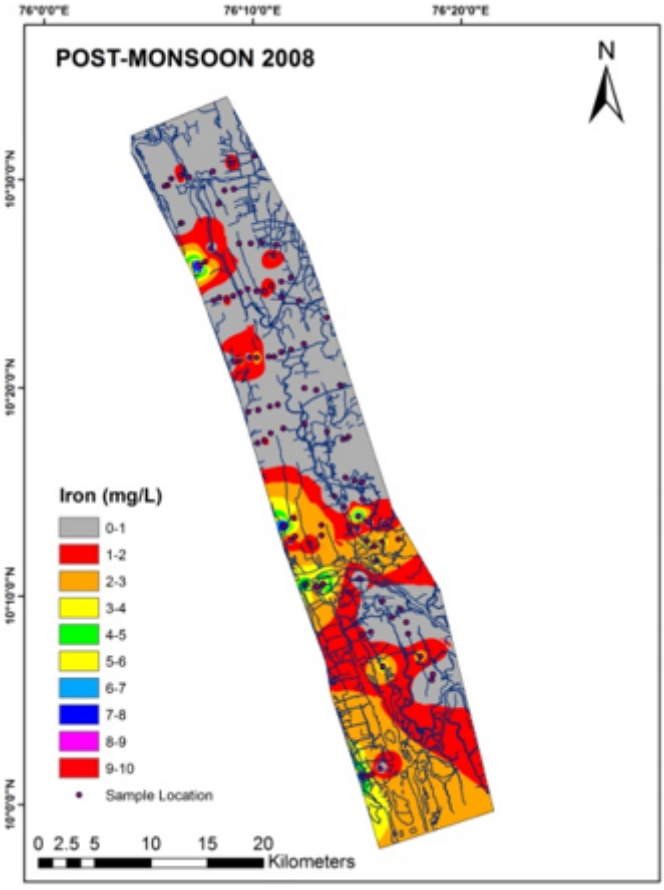

Figure 18

Iron (Fe) content of the water samples in the post-monsoon season

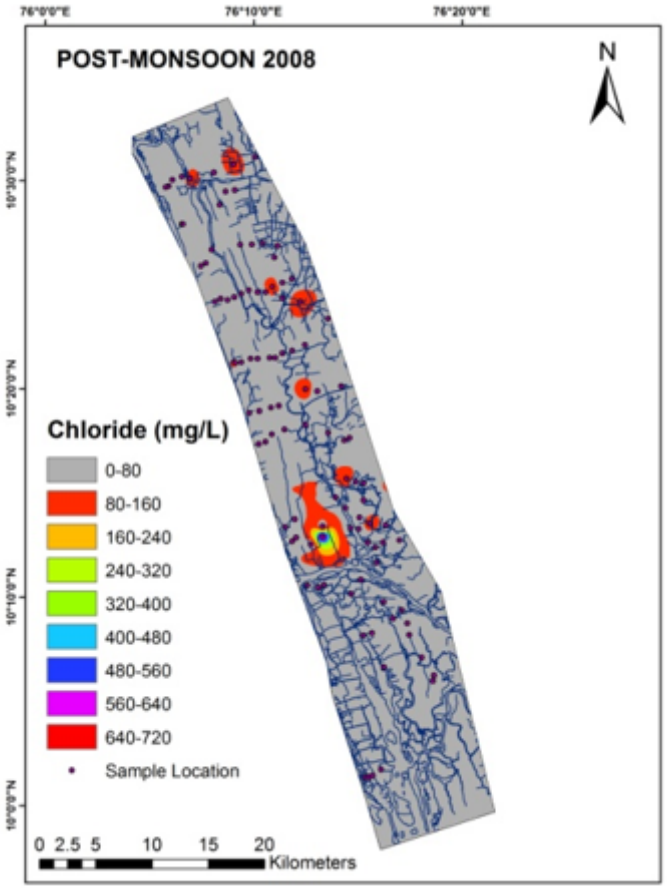

Figure 19

Chloride (Cl-) content of the water samples in the post-monsoon season

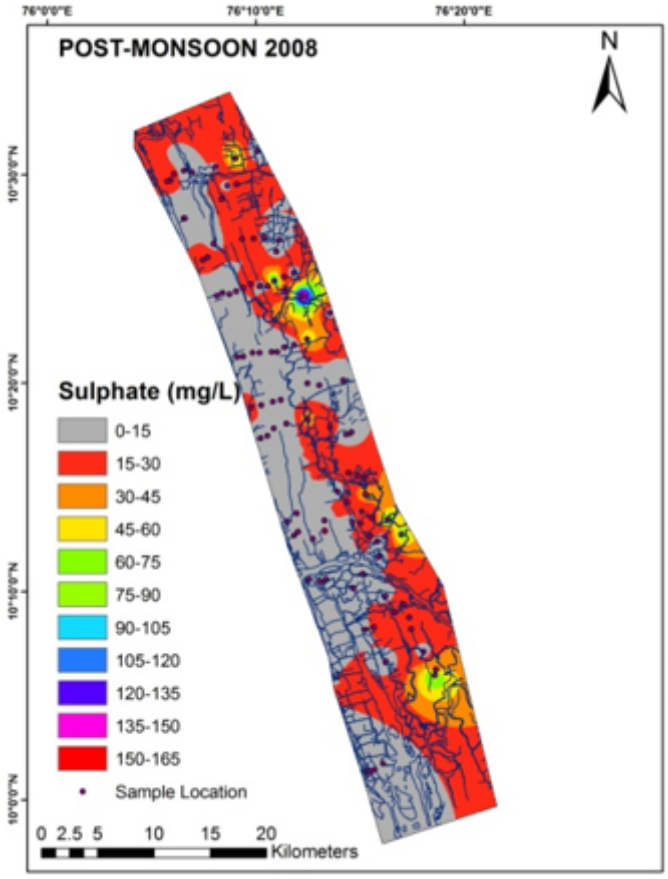

Figure 20

Sulfate (SO42-) content of the water samples in the post-monsoon season

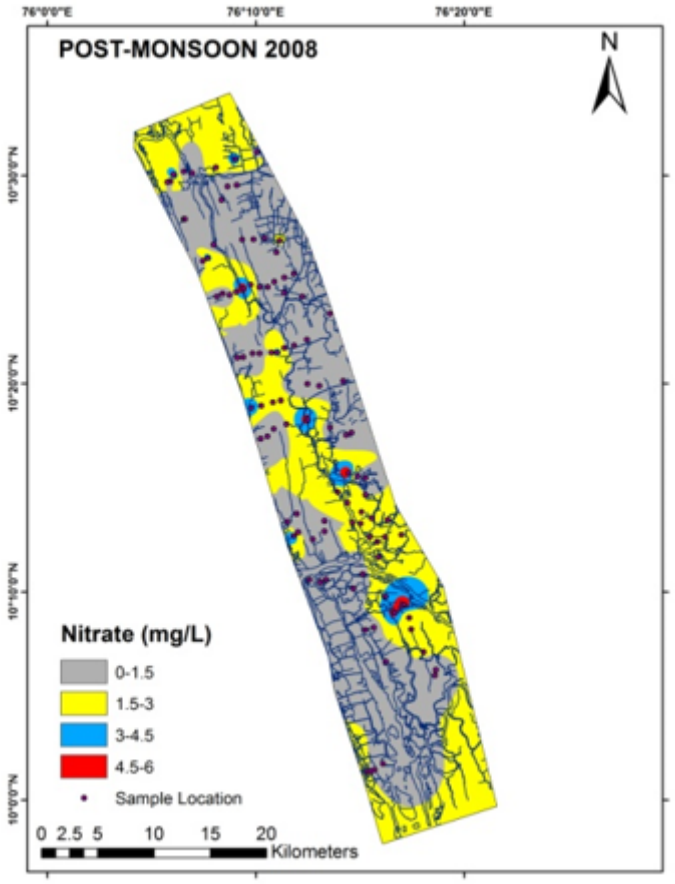

Figure 21

Nitrate (NO3-N) content of the water samples in the post-monsoon season

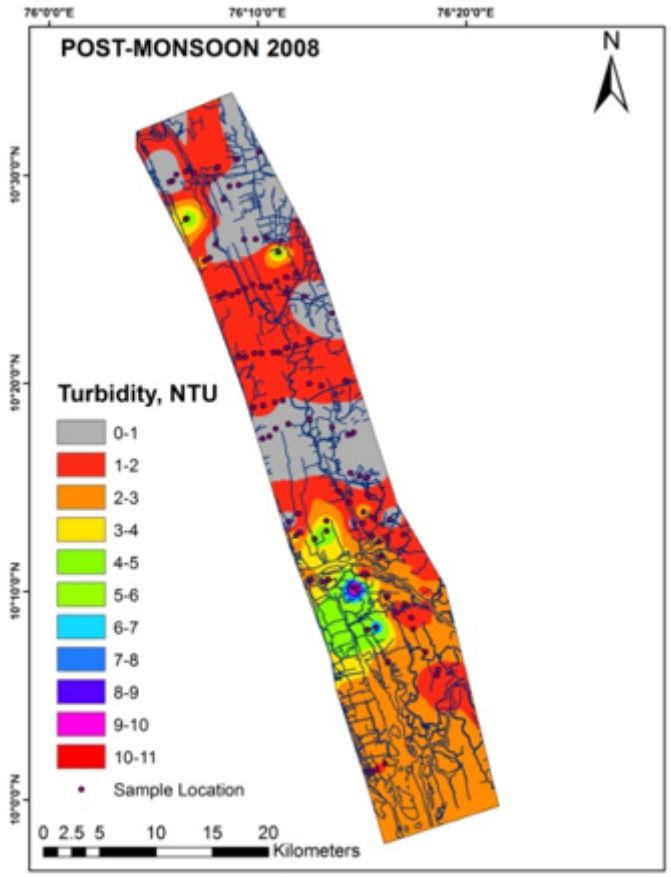

Figure 22

Turbidity of the water samples in the post-monsoon season

Supplementary Files

This is a list of supplementary files associated with this preprint. Click to download.

- Crosssectionalprofiles.docx
- VerticalElectricalSounding.docx